Analyses of Pre-Swirl Spray Formation and Its Breakup Processes of D.I. Gasoline Spray

Jeekuen LEE and Keiya NISHIDA

University of Hiroshima, 1-4-1 Kagamiyama, Higashi-Hiroshima 739-8527, Japan

The breakup and atomization processes of the pre-swirl spray, which is formed before the hollow-cone spray from a high-pressure swirl-type D.I. gasoline injector, were investigated experimentally. A microscopic imaging technique was applied to get the spatially high-resolution LIF tomograms of the pre-swirl spray. The droplet size and the individual droplet's velocity were obtained by applying the imaging processing and the particle tracking techniques, respectively. The breakup regime of the pre-swirl spray includes the following four stages in the order of changes: (a) liquid column stage (SOI-0.13 ms); (b) liquid blob stage (0.13-0.4 ms); (c) ligament stage (0.4-0.6 ms); and (d) large-sized droplet stage (0.6 ms-after). The stages (a), (b) and (c) belong to the primary breakup process, and the stage (d) belongs to the secondary breakup process.

1. Introduction

Currently, the most widely utilized D.I. gasoline injector is the single-fluid, single exit-orifice and high-pressure swirl-type injector. This high-pressure swirl-type injector produces a hollow-cone spray by imparting the swirling motion to the fuel inside the injector. In this injector design, the fuel flows through a series of the tangential slots into the swirl chamber. The fuel spreads out as a thin conical sheet leaving the injection hole owing to the centrifugal force that enhances atomization. As a result, the high-pressure swirl-type injectors generally provide a fine and widely dispersed fuel spray with moderate injection pressure.

Recently, several researches have been devoted to the characterization of the transient atomization of the high-pressure swirl-type injector [1-4]. A review of the previous researches mentioned above indicates that the spray initially emanating from a high-pressure swirl-type injector is not a hollow-cone spray but a liquid column or blob that is changed into a pre-swirl spray, after which a hollow cone spray with a certain cone angle is formed. In addition, the pre-swirl spray exhibits significantly large droplets with high axial velocity so that the pre-swirl spray impinges on the piston surface, resulting in the main source of unburned hydrocarbon (HC) emissions [1,5]. However, in spite of the great impact of the pre-swirl spray on the mixture preparation processes and engine-out emissions, the recent researches [1,2] are limited to the simple observation of their structural behaviors, not providing the quantitative results such as droplet size and velocity. Particularly, the separate characterization of the pre-swirl spray from the main spray was not made because the pre-swirl spray shows significant cycle-to-cycle variability, and moreover the pre-swirl spray are followed by the main spray moving with high axial velocity.

In this study, the characterization of the breakup and atomization processes of the pre-swirl spray, which is formed before the hollow-cone spray from a high-pressure swirl-type D.I. gasoline injector, was carried out under different ambient pressure conditions. A microscopic imaging technique was applied to get the spatially high-resolution LIF tomograms of the pre-

swirl spray. The droplet size and the individual droplet's velocity were obtained by applying the imaging processing and the particle tracking technique, respectively.

2. Experimental Setup and Conditions

Figure 1 shows the experimental setup for the pre-swirl spray imaging. The fuel injection system consisted of a constant volume chamber, a fuel injector and an injector driver. The constant volume chamber could be pressurized up to 10 MPa with a nitrogen gas. Fuel is supplied under constant pressure from an accumulator pressurized with a nitrogen gas. The fuel injection timing and duration were controlled by a delay pulse generator (Stanford Research System, Model DG535) that could be set in 5ps increment.

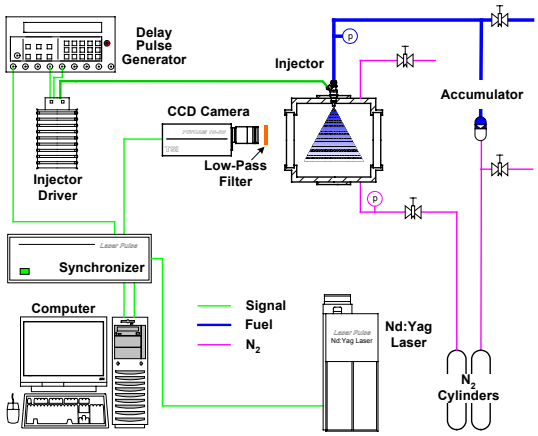

Fig. 1 Experimental setup for pre-swirl spray imaging

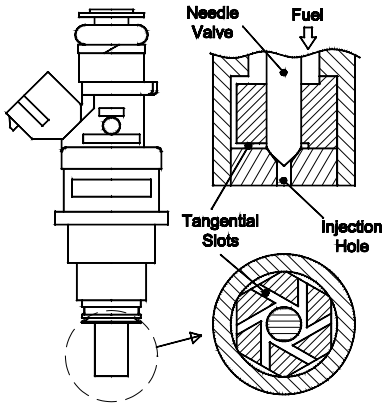

Fig. 2 Details of injector swirl tip

The spray imaging system consisted of an Nd:YAG laser, a CCD camera coupled with an optical low-pass filter. For the illumination of the fuel spray, the Nd:YAG laser (LASERPULSE, wavelength of 532 nm, pulse width of 6 ns, power of 25 mJ), which forms a sheet 1 mm thick by cylindrical lenses, was used as a light source for taking the pre-swirl spray tomogram. The optical low-pass filter was used to discriminate the Mie scattering and LIF signal from the pre-swirl spray and subsequently to take the LIF tomogram of the pre-swirl spray. The LIF signals from the pre-swirl spray droplets were recorded with a high-resolution CCD camera (TSI Inc., PIVCAM 10-30, 1000x1016 pixels, 8-bit in grayscale level), fixed with a 60 mm focal length Nikon Micro Nikkor lens for getting the spray tomograms with spatially high resolution. The physical size of the image obtained was 12.25x12.65 mm^2 in horizontal and vertical, respectively, yielding a spatial resolution of 0.01246 mm per pixel with the same aspect ration.

The fuel injector used was a high-pressure swirl-type D.I. gasoline injector that is widely used in the D.I. gasoline engines, particularly with a wall-guided combustion system. Schematic diagrams of the injector and details of the injector tip including the tangential slots are shown in Fig. 2. The injector has a press-fitted swirl tip in which an in-swirl chamber composed of the six equally spaced tangential slots is constituted. These tangential slots give the injecting fuel an angular momentum, resulting in producing a relatively well-atomized hollow-cone spray. However, due to the geometric arrangement of the in-swirl chamber for guaranteeing the fuel passage, an unavoidable non-swirling volume usually called sac or dead volume, in which the fuel leaves the injector without the angular momentum, is in existence between the needle valve seat and the exit of the tangential slots. The hole diameter of the injector was 0.5 mm, and the length to diameter ratio of the injection hole (l_n/d_n) was 2.3.

The pre-swirl spray imaging was made at a fixed fuel injection pressure of 5.0 MPa and at

two different ambient pressures of 0.1 and 0.4 MPa under room temperature. The pre-swirl sprays were visualized at several timings from the start of injection (hereafter SOI) until the pre-swirl sprays were not visualized anymore. The width of an injection control pulse, generated by a delay pulse generator, was 0.88 ms. The actual injection duration, which also meant the actual end of injection, was 1.25 ms. The injection quantity was 7.24 mg/st.
The fuel used was dry-solvent whose physical properties are very close to those of a commercial gasoline, particularly in density and surface tension. For the LIF spray imaging, rhodamine B was used as a fluorescent dye, of which final concentration was 50 ppm. All pressure notations used in this paper are given in terms of absolute pressure. The injector axis is defined as the axial direction, Z, and the radial direction was defined as R. The origin is located at the injector tip.

3. Typical Spray Structure Formed by High-Pressure Swirl-Type Injector

Figure 3 shows the Mie scattering images of the whole spray (left-hand side) and the LIF tomograms of the pre-swirl spray (right-hand side), each of which was imaged at a different injection event, at 0.6 ms from SOI at ambient pressure of 0.1 MPa. In the whole spray images, the pre-swirl spray, located in the downstream of the main spray, is clearly identified and shows a liquid blob shape, resulting from the higher scattering light intensity. However, the LIF tomograms of the pre-swirl spray reveal that the pre-swirl spray is composed of the large-sized droplets with various shapes, differently from its appearance shown in the Mie scattering images of the whole spray. These pre-swirl sprays show completely different spray characteristics, including the spray tip penetration, cone angle and SMD, from the main spray with a hollow-cone shape. This indicates that the pre-swirl spray should be characterized separately from other sprays; however, this is seldom done in practice because of the measurement complexity and the requirement of precise time-windowing for the droplet sizing and velocity analysis.

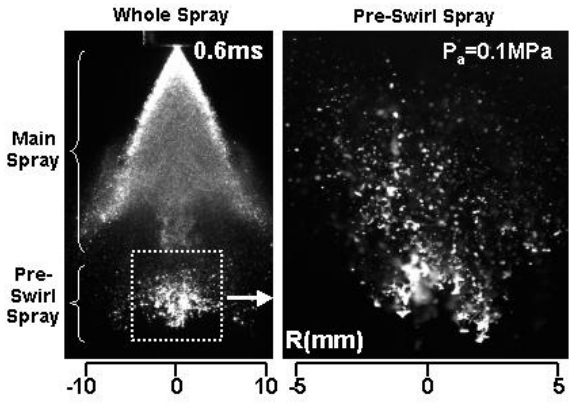

Fig. 3 Mie scattering images of whole spray (left-hand side) and LIF tomograms of pre-swirl spray (right-hand side) at 0.6 ms from start of injection at ambient pressure of 0.1 MPa.

4. Results and Discussion

4.1. LIF Tomograms of Pre-Swirl Spray and Its Breakup Process

Figure 4 shows a sequence of the LIF tomograms of the pre-swirl spray from SOI at ambient pressure of 0.1 MPa. These tomograms were imaged at a different injection event from each other due to the very precise time interval as short as 0.05 ms between image frames and the very high spatial resolution as large as 1000x1016 pixels. As described before, at SOI, the liquid column emerges first, and it develops without expanding in the radial direction; as time elapses, the liquid column expands in radial direction due to the increased resistance by the ambient air and finally changes into the liquid blob that is shown in the LIF tomogram at 0.3 ms from SOI. Continuously, the liquid blob begins to disintegrate into the small-sized liquid blob and the long-ligaments at the outer boundary, as shown at 0.35 and 0.4 ms from SOI.

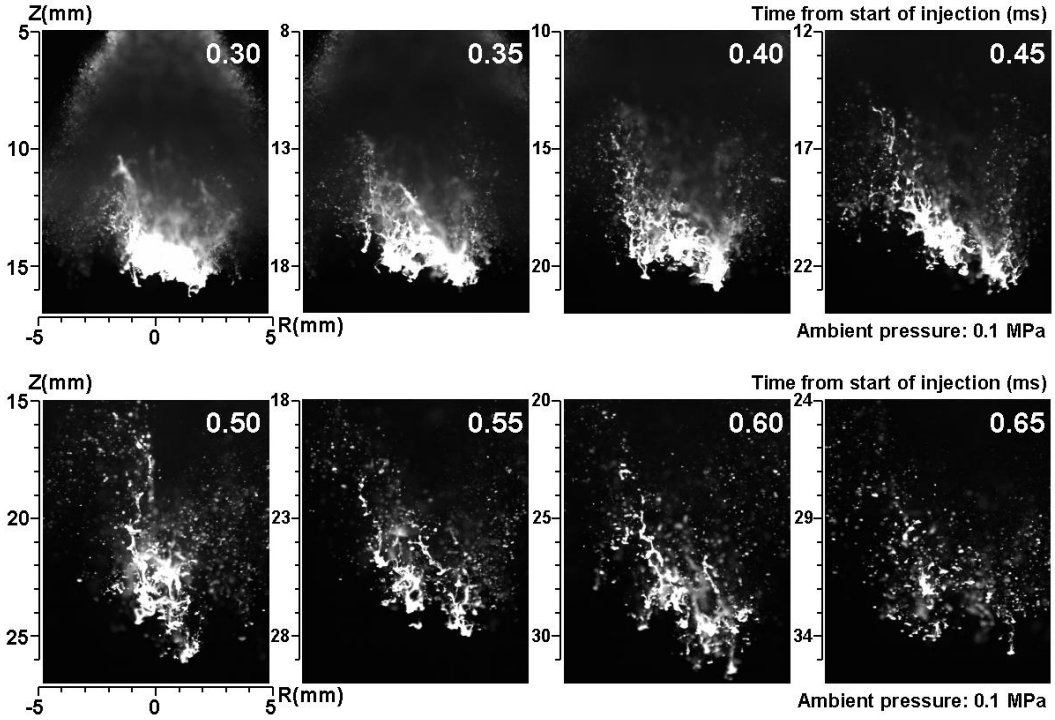

Fig. 4 LIF tomograms of pre-swirl spray with time from start of injection at ambient pressure of 0.1 MPa

At 0.45 ms from SOI, many long-ligaments are produced in the periphery and at the upstream of the pre-swirl spray. However, the central parts of the pre-swirl spray are still showing the liquid blob shape with a decreased size though its internal part shows the porous shape. At 0.5 and 0.55 ms from SOI, the very long-ligaments parallel to the axial direction and its disintegration into the short-ligaments occurs consecutively; the liquid blob in the central part of the pre-swirl spray also nearly breaks down into the small-sized liquid blob or the very large-sized droplets. At 0.6 ms from SOI, the long-ligaments change into the small-sized ligaments, and the liquid blob does not observed in the central part of the pre-swirl spray anymore. At 0.65 ms from SOI, the large-sized droplets with a non-spherical shape are produced through the multi-separation of the long-ligaments. Spatial distribution of the disintegrated droplets is non-uniform with a low number density. These large-sized droplets will disintegrate into the small-sized droplets through the secondary atomization until the aerodynamic forces and the surface tension forces are equal or the droplets will impinge on the piston surface in the engine environments.

Considering the breakup regime, the liquid blob produced from the radial expansion of the liquid column changes into the long-ligaments; consecutively they disintegrate into the large-sized droplets with a very irregular shape. In particular, the breakup regime of the long-ligaments showing the multi-separation is noteworthy to understand the droplet formation process. Through the careful consideration on the breakup processes of the pre-swirl spray, it is concluded that the breakup regime of the pre-swirl spray can be classified into following four stages in the order of changes: (a) liquid column stage from SOI to 0.13 ms (see reference [2]); (b) liquid blob stage (0.13-0.4 ms); (c) ligament stage (0.4-0.6 ms); and (d) large-sized droplet stage (0.60 ms-after).

4.2. Droplet Sizing of Pre-Swirl Spray Using Image Processing

In order to characterize the breakup regime of the pre-swirl spray, the image processing

technique was introduced to determine the droplet size of the pre-swirl spray, and it was applied to analyze using the LIF tomograms shown in Fig. 4.

Figure 5 shows the procedure of the image processing for the pre-swirl spray droplet sizing. First, the noise incorporated in the image is removed by applying the low-pass filter, and then the noise-removed image changes into a binary image by applying the threshold level. In this research, the threshold level of 160 in 8-bit grayscale level, which was decided through the preliminary test of the single droplet acquired at the same condition with the LIF tomogram of the pre-swirl spray, was applied. Using the binary image, the droplet sizing, including the calculation of the area occupied by the droplet and ascertaining of the droplet centroid and the edge, was made. In the droplet sizing, the area occupied by one pixel is 0.0125x0.0125 mm^2, which is corresponding to the sectional area of spherical droplet with diameter of 14.0 μm. By measuring the particle image reticle for the calibration of particle sizing, the results of the image processing were verified with the results of an LDSA (laser droplet size analyzer, TONICH Computer Co., Japan, 1400A, beam diameter of 8 mm, sensing time of 0.5 ms, measurement range of 1.4-1000 μm), which is one of well-known laser diffraction based droplet sizing technique similar to the Malvern particle sizer.

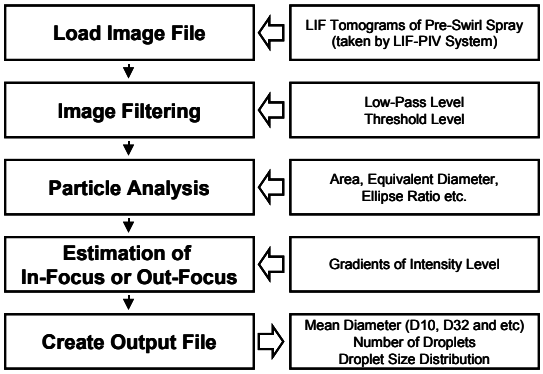

Fig. 5 Procedure of image processing for pre-swirl spray droplet sizing

4.3. Temporal Variation of Droplet Size of Pre-Swirl Spray

Figure 6 shows the temporal variation of the SMD of the pre-swirl spray from SOI at ambient pressures of 0.1 and 0.4 MPa. Within 0.6 ms from SOI, the extremely high SMD, which is completely different from the results proposed by Shelby et al. [1] who made the pre-swirl spray droplet sizing using the laser diffraction based technique, are shown, after which the SMD shows a significantly small value. These high SMDs within 0.6 ms are associated with the presence of the liquid blob expanded radially, though the large-sized droplets around the liquid blob are involved in the estimation of the SMD. The SMD of the pre-swirl spray during 0.3-0.4 ms, when the liquid blob breakup behavior is dominated, shows very higher value on the order of 3500 μm with very larger scatter, and then it steeply decreases during 0.4-0.6 ms when the breakups of the long-ligament and the small-sized liquid blob are the main processes. In particular, the SMD shows very dramatic change during this duration, which means that the long-ligament and the small-sized liquid blob are in the very unstable state so that they breakup rapidly during this period as short as 0.2 ms. In addition, the SMD at high ambient pressure shows a little higher value than that at low ambient pressure.

Figure 7 shows the temporal variation of the SMD of the pre-swirl spray from 0.6 ms when the large-sized droplet begins to be produced at ambient pressures of 0.1 and 0.4 MPa. In addition, the SMD variations measured by the image processing are compared with the results measured by the LDSA. In the LDSA measurement, the presence of the pre-swirl spray was identified with the variation of the transmittance just before the pre-swirl spray. The LDSA measurement was made more than 10 times at the axial distances of 20, 30 and 40 mm, and the data plotted here is the average value at the given condition. The SMD, measured by the image processing technique, steeply decreases with time after 0.6 ms from SOI, and, at the actual end of injection of 1.25 ms, it shows 105 and 65 μm at ambient pressures of 0.1 and 0.4 MPa, respectively.

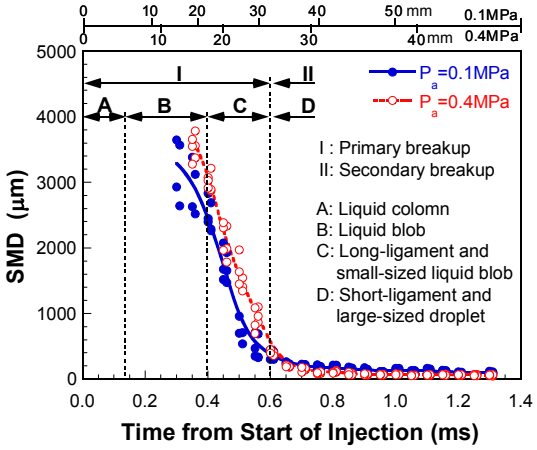

Fig. 6 Temporal variation of SMD of pre-swirl spray at ambient pressures of 0.1 and 0.4 MPa (data for 0.3-1.3 ms)

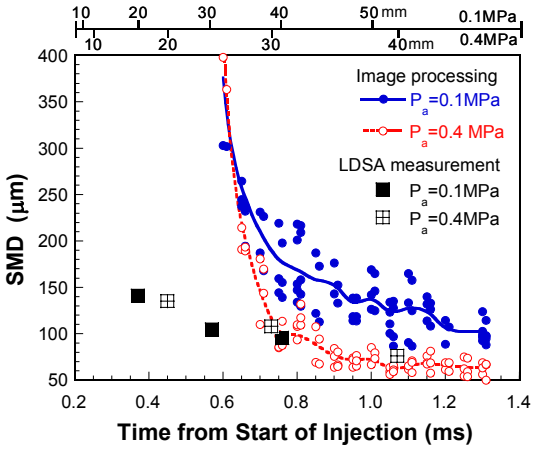

Fig. 7 Temporal variation of SMD of pre-swirl spray at 0.1 and 0.4 MPa (data for 0.6-1.3 ms ordinate enlarged from Fig. 6)

In addition, the SMD and the degree of its scatter show higher value at 0.1 MPa than that at 0.4 MPa. This smaller SMD at high ambient pressure results from the increased aerodynamic forces due to the increased ambient pressure. The SMD, measured by the LDSA, shows a considerable difference from the results of the image processing within 0.6 ms from SOI, namely, at the axial distances of 20 and 30 mm for ambient pressure of 0.1 MPa and at 20 mm for ambient pressure of 0.4 MPa, respectively. It is because the upper measurement limit in the LDSA is constrained to 1000 μm, while, as confirmed in Fig. 4, the size of the liquid blob is at least over 1000 μm. After 0.8 ms from SOI when the droplets begin to be produced actively, the SMD measured by the LDSA is similar to the image processing result, especially at high ambient pressure of 0.4 MPa. This result indicates that the laser diffraction based droplet sizing technique is applicable after 0.8 ms when the pre-swirl spray begins to comprises mainly large-sized droplets within the measurable range. Resultantly, the comparisons between the image processing technique and the LDSA measurement well point out that the LDSA measurement of the pre-swirl spray should be applied restrictively only at the larger axial distance where the pre-swirl spray consists of the droplets within a measurement range.

4.4. Velocity Measurement of Pre-Swirl Spray Using Particle Tracking Technique

The 2-frame particle tracking technique, which is one of the oldest ways to evaluate the velocity and of which the theory and practical technique is well introduced in many literatures [7-9], was introduced to calculate the large-sized non-spherical droplet's velocity. The experimental setup is the same as Fig. 1. For the illumination of the pre-swirl spray, the dual firing of the Nd:YAG laser was made. The 1 mm thick laser light sheet exposes the spray two times, with a small time interval of 0.01 ms between the pulses. As a result, the consecutive two images were recorded by a high-resolution frame-straddle CCD camera. The obtained images were transferred to a computer, and then 2-dimensional velocity vectors

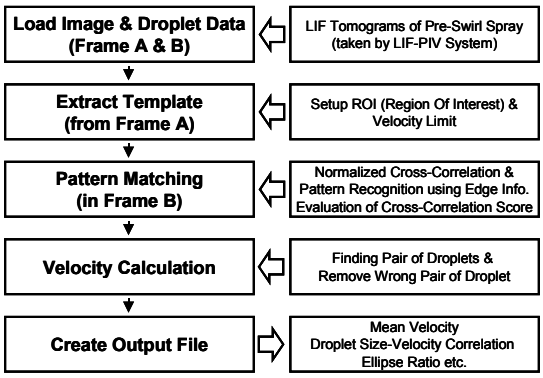

Fig. 8 Procedure of particle tracking using two-frame LIF images for calculating individual droplet velocity

of the pre-swirl spray were calculated by using a 2-frame PTV technique, based on the cross-correlated sub-regions of the frame-straddle images, as illustrated in Fig. 8. The detection of the particles, including the centroid and the outer boundary of the individual droplet, was made by referring to the image processing results shown in Section 4.3.

4.5. Temporal Variation of Velocity of Pre-Swirl Spray

Figure 9 shows the velocity vector plots of the pre-swirl spray (represented as arrows) and the sizes of the individual droplet (represented as open circles) at 0.6 and 0.8 ms from SOI at ambient pressure of 0.1 MPa. Almost all of the droplets show high axial and low radial velocities mainly due to the inherent characteristic of the pre-swirl spray that is constituted by the fuel leaving the injector without the swirl components. At 0.6 ms from SOI, relatively large-sized droplet appears in the central part of the pre-swirl spray. As time elapses, at 0.8 ms from SOI, the droplet size decrease so that the number density of the pre-swirl spray increases.

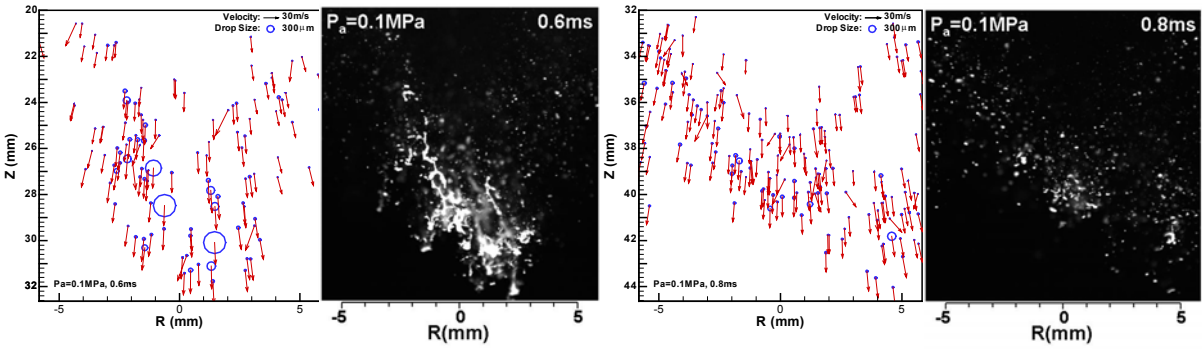

(a) 0.6 ms from SOI (b) 0.8 ms from SOI

Fig. 9 Velocity vector plots of pre-swirl spray (represented as arrows) and size of individual droplet (represented as open circle) at ambient pressure of 0.1 MPa

Figure 10 shows the temporal variations of the mean axial velocity of the whole pre-swirl spray and the axial velocity of the leading edge of the pre-swirl spray at ambient pressure of 0.1 MPa. Here the leading edge of the pre-swirl spray was decided by using the three or five relatively large-sized droplets over 50 μm, depending upon the spray number density around the leading edge of the pre-swirl spray. The mean axial velocity and the axial velocity of the leading edge of the pre-swirl spray decrease linearly with time from SOI, and the axial velocity of the leading edge of the pre-swirl spray is higher than the mean axial velocity of the pre-swirl spray.

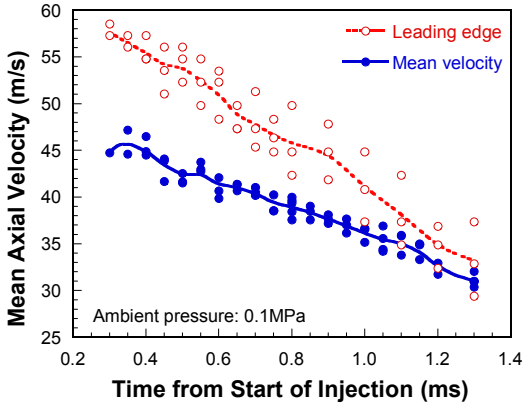

Fig. 10 Mean axial velocity distributions at ambient pressure of 0.1 MPa

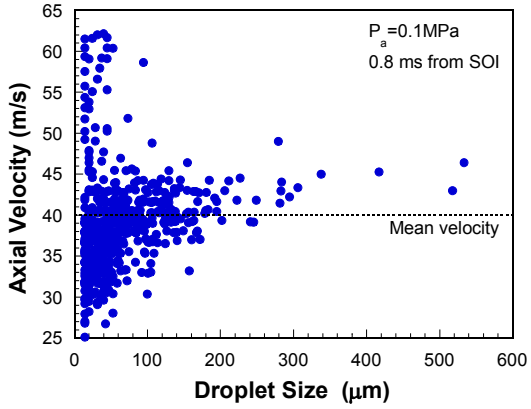

Fig. 11 Correlation between axial velocity and droplet size at 0.8 ms from SOI and at 0.1 MPa

The difference between the two velocities is larger around 0.3 ms from SOI, and then it decrease with time from SOI and shows similar values at the actual end of injection of 1.25 ms. The main reason for the difference between the two velocities is that the large- and small-sized droplets around the pre-swirl spray transfer rapidly their axial momentum to the ambient air. Figure 11 shows the correlation between the axial velocity and the droplet size at 0.8 ms from SOI at ambient pressure of 0.1 MPa. The small-sized droplets show a very broad velocity range, while the large-sized droplets show a relatively narrow velocity range. The large scattering of the small-sized droplet velocity is related with a relatively short time scale maintaining their axial momentum. The large-sized droplets over 200 μm show analogous axial velocity to the mean velocity of the whole pre-swirl spray. However, despite the velocity-dependency of some large-sized droplets, it is hard to say that the droplet velocity of the pre-swirl spray has a strong correlation with the droplet size.

5. Conclusions

The breakup and atomization processes of the pre-swirl spray, which is formed before the hollow-cone spray from a high-pressure swirl-type D.I. gasoline injector, were investigated. The results are summarized as follows.

1. A microscopic imaging technique was applied to get the spatially high-resolution LIF tomograms of the pre-swirl spray. The droplet size and the individual droplet's velocity were obtained successfully by applying the imaging processing and the particle tracking techniques, respectively.
2. The breakup regime includes the following four stages in the order of changes: (a) liquid column stage (SOI to 0.13 ms); (b) liquid blob stage (0.13-0.4 ms); (c) ligament stage (0.4-0.6 ms); and (d) large-sized droplet stage (0.6 ms- after).
3. The SMD of the pre-swirl spray during the liquid blob stage (0.13-0.4 ms) shows large value with the wide scattering, and then it steeply decreases during the ligament stage (0.4-0.6 ms) with a period as short as 0.2 ms. In addition, the SMD of the pre-swirl spray during the large-sized droplet stage (0.6-0.8 ms) gradually decreases with time, and it shows smaller value at 0.4 MPa than that at 0.1 MPa, resulting from the increased aerodynamic forces due to the increased ambient pressure.
4. The leading edge velocity decreases with time and approaches the similar value to that of the mean velocity value. The small-sized droplets show a very broad velocity range, while the large-sized droplets show a relatively narrow velocity range.

Acknowledgement
The authors would like to thank Dr. Laurent Zimmer at National Aerospace Laboratory of Japan for his valuable discussion and for providing us with the literature on the particle tracking velocimetry (PTV) algorithm.

References

[1] Shelby, M.H. et al., SAE Paper 980160, 1998
[2] Lee, J.K. and Nishida, K., SAE Paper, 2003-01-1809, 2003
[3] Chryssakis, C.A. et al., SAE Paper 2003-01-0007, 2003
[4] Lee, J.K. and Nishida, K., SAE Paper 2003-01-1115, 2003
[5] Joh, M.O. et al., SAE Paper No. 2001-01-3668, 2001
[6] Parrish, S.E. and Farrell, P.V., SAE Paper 970629, 1997
[7] Zimmer, L. et al, ILASS-Europe, July 5-7, 1999, Toulouse, France
[8] Zimmer, L., Lecture Series 2000-1, von Karman Institute for Fluid Dynamics, 2000
[9] Raffel, M. et al., Particle Image Velocimetry-A Practical Guide, Springer, 1998